Supplemental Materials

Supplemental Figures

Figure S1

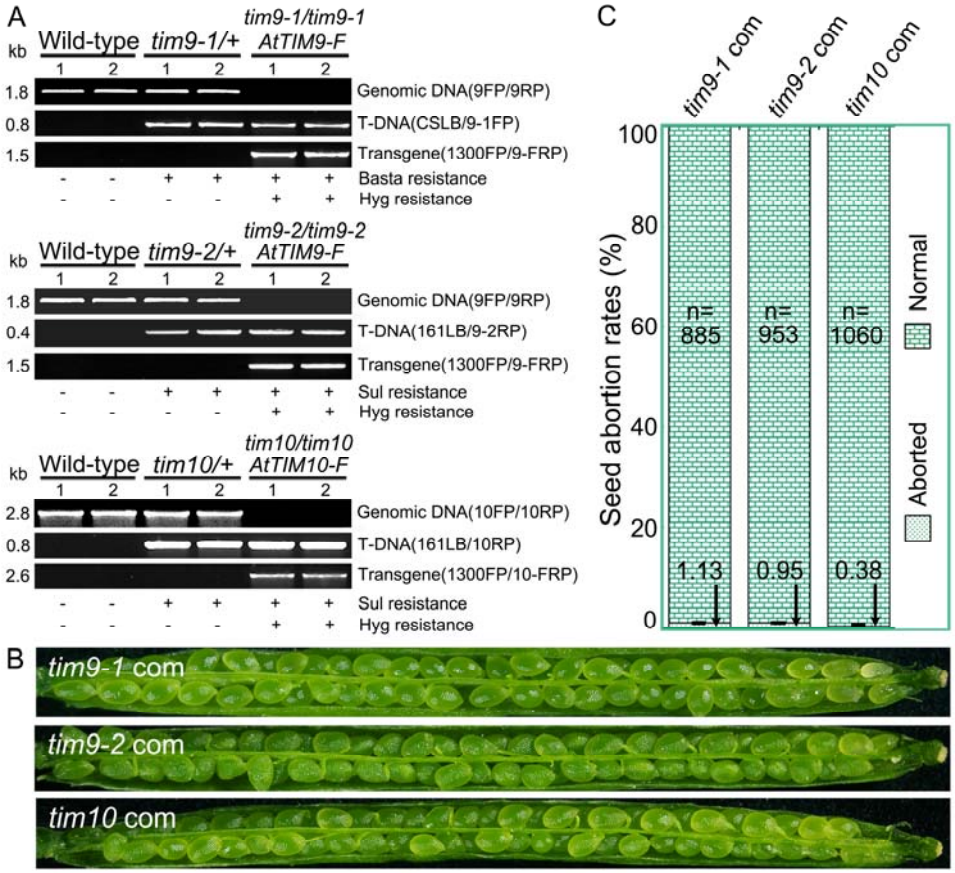

Figure S1 Complementation assays of *AtTIM9* and *AtTIM10* mutants. A, Genotypic analysis of *tim9-1/+*, *tim9-2/+* and *tim10/+* mutants, and genotypic confirmation of the T3 generation homozygous transgenic mutant plants in complementation experiments. Two lanes for each genotype represent two different lines of each sample. *AtTIM9-F* and *AtTIM10-F*, the full sequence of *AtTIM9* and *AtTIM10* genes. B, Phenotype of the siliques in T3 homozygosis transformed complemental (com) plants based on the *tim9-1/+*, *tim9-2/+* and *tim10/+* mutants. C, Seed abortion rates of T3 homozygosis transformed complemental plants based on the *tim9-1/+*, *tim9-2/+* and *tim10/+* mutants. Total numbers (n) of counted seeds from each mutant are listed on the top of the histogram, and the values of seed abortion rate are shown on the bottom.

Figure S2

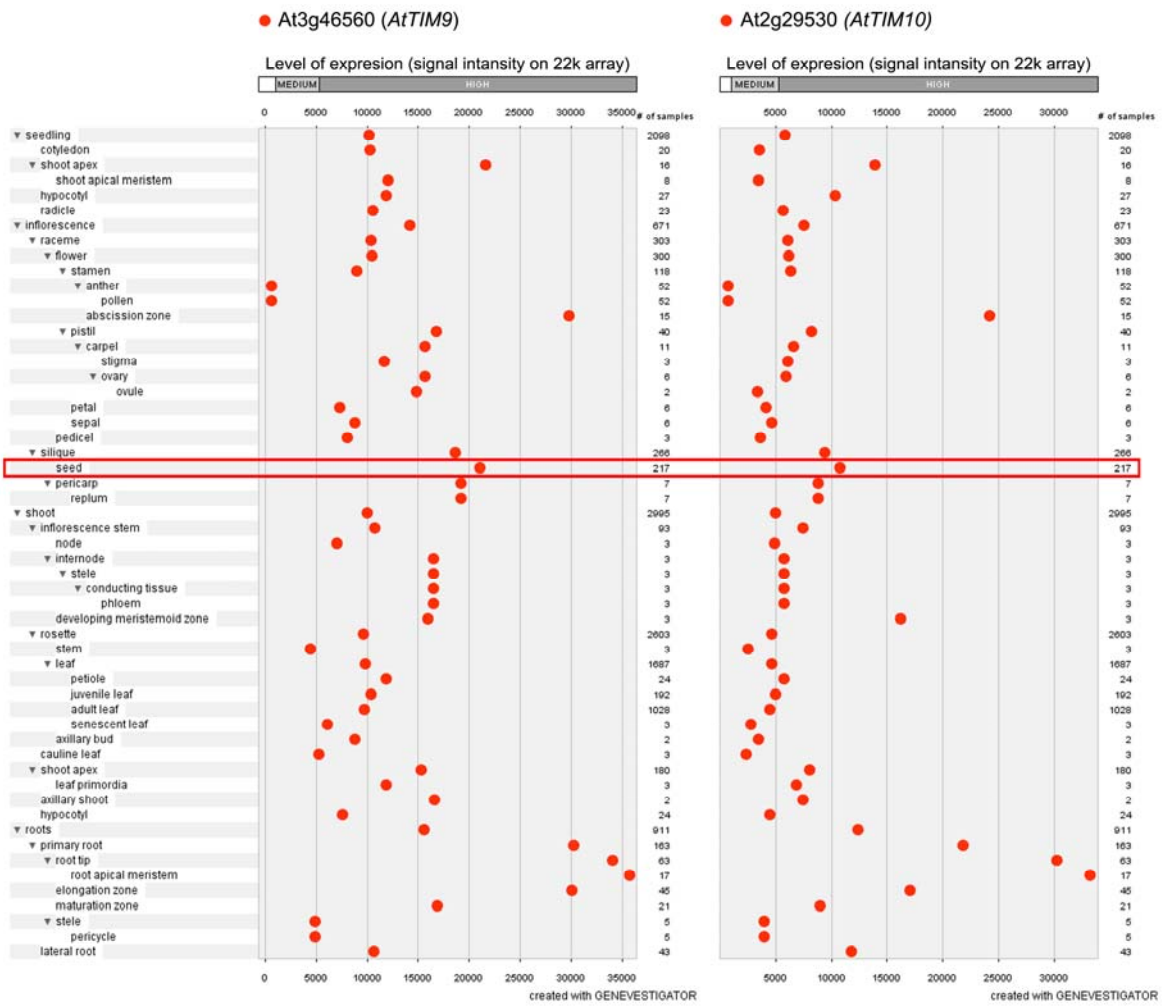

Figure S2 Expression data of *AtTIM9* and *AtTIM10* from public databases. *AtTIM9* and *AtTIM10* temporal and spatial expression data were extracted from Genevestigator v3. The x-axis indicates expression levels.

Figure S3

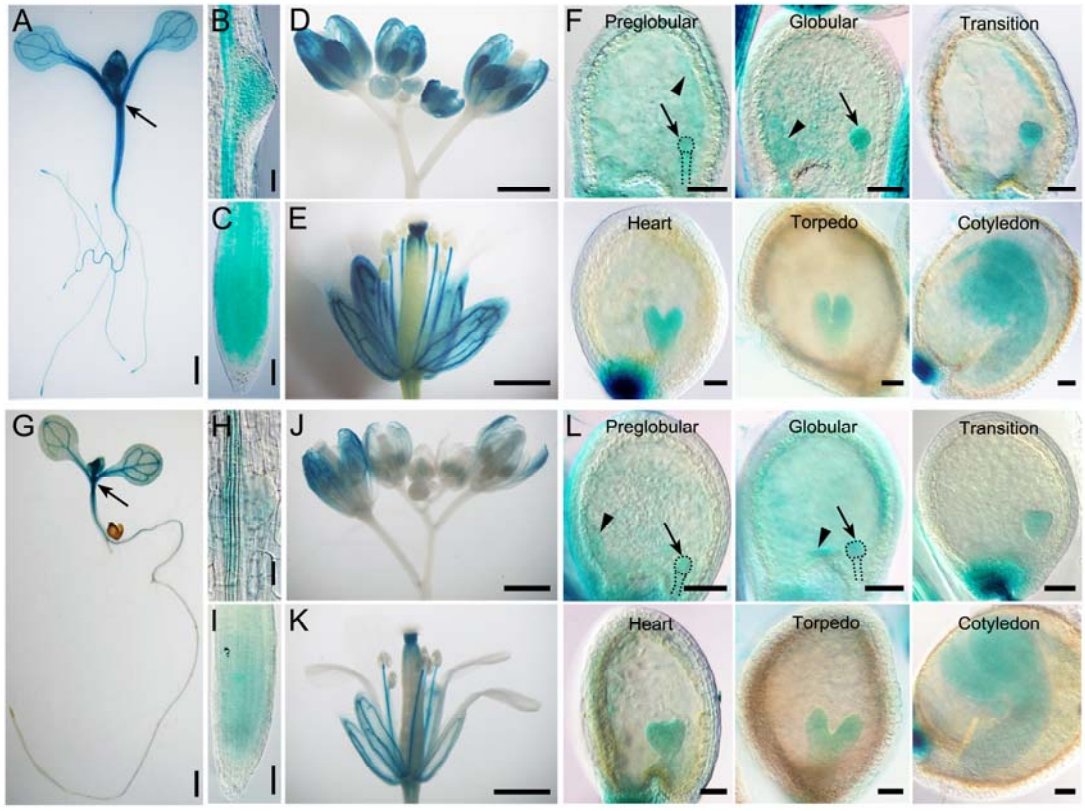

Figure 3 GUS staining in the *ProAtTIM9*::GUS and *ProAtTIM10*::GUS transgenic plants. (A-F) Showing the temporal and spatial expression of *AtTIM9* gene; (G-L) Showing the temporal and spatial expression of *AtTIM10* gene. (A and G) The 2-week-old seedlings. Arrows indicate the SAM. Bars=1mm. (B and H) The lateral root primordia of 2-week-old seedlings. Bars=50μm. (C and I) The root tips of 2-week-old seedlings. Bars=50μm. (D and J) The inflorescences with immature and mature flowers. Bars=1mm. (E and K) The mature flowers. Bars=1mm. (F and L) The ovules at different developing stages: preglobular, globular, transition, heart, torpedo and cotyledon stages. Arrows and arrowheads showing the embryos and endosperm in the olvules, respectively. Bars=50μm.

Figure S4

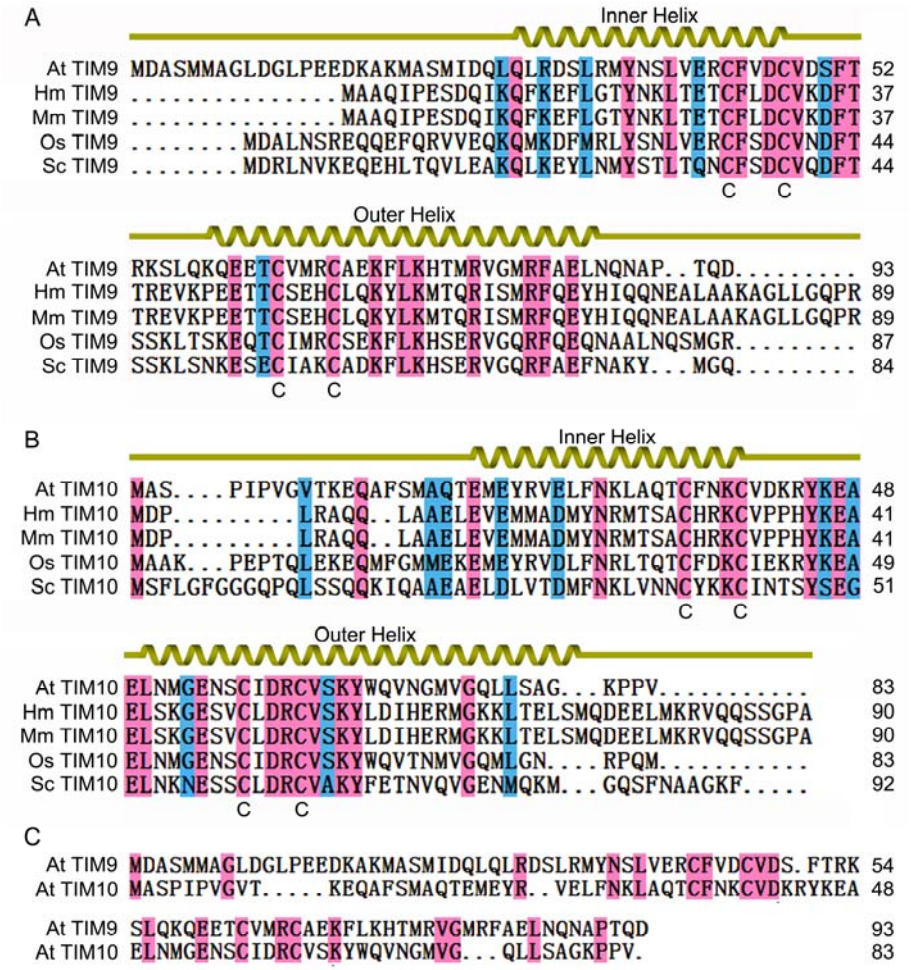

Figure S4 AtTIM9 and AtTIM10 are conserved among eukaryote. A and B, Amino acid sequence alignments of AtTIM9 and AtTIM10 with homologues from other organisms are presented. C, Amino acid sequence alignments between AtTIM9 and AtTIM10. Identical residues occurring in all organisms are indicated in pink and similar residues are indicated in blue. At, *Arabidopsis thaliana*; Hm, *Homo sapiens*; Mm, *Mus musculus*; Os, *Oryza sativa*; Sc, *Saccharomyces cerevisiae*. The National Center for Biotechnology Information accession numbers for TIM9 and TIM10 proteins discussed in this article and the supporting information are: AtTIM9 (GI: 332644651), HmTIM9 (GI: 12230191), MmTIM9 (GI: 12230178), OsTIM9 (GI: 90110081), ScTIM9 (GI: 12230137), AtTIM10 (GI: 330253173), HmTIM10 (GI: 49065657), MmTIM10 (GI: 49065658), OsTIM10 (GI: 5107214), and ScTIM10 (GI: 12230145).

Figure S5

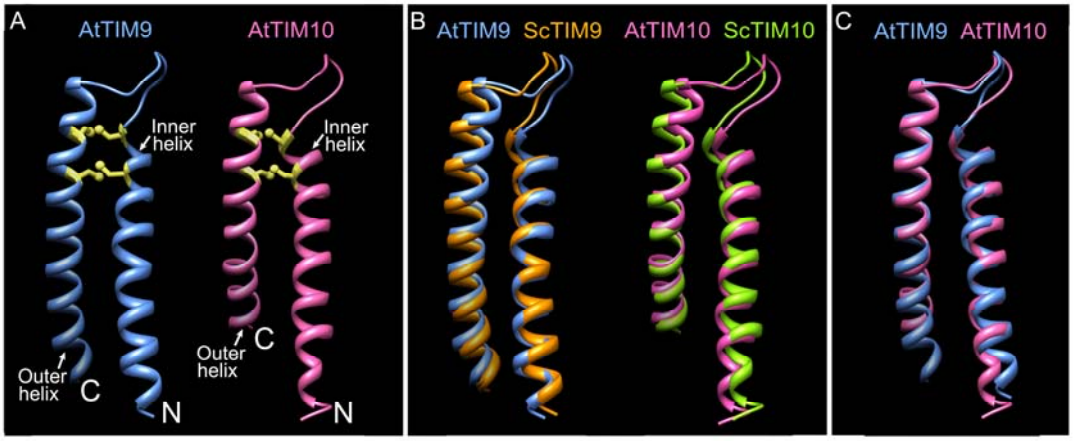

Figure S5 Homology modeling of AtTIM9 and AtTIM10. A, Ribbon diagrams of the AtTIM9 (blue) and AtTIM10 (pink) structure are predicted by Swiss-Model. The depicted individual AtTIM9 and AtTIM10 forming hairpin-like structures are brace by two intramolecular disulfide bonds shown as yellow stick representation. B, Comparison of AtTIM9 and AtTIM10 with the subunits of the yeast Tim9-Tim10 complex (PDB ID 3DXR). AtTIM9 (blue) is superimposed on ScTIM9 (orange), and AtTim10 (pink) is superimposed on ScTIM10 (green). C, Superposition of AtTIM9 (blue) and AtTIM10 (pink) structures. Proteins crystal structure data from this article can be found in the RCSB Protein Data Bank database under the accession number 2BSK (*Homo sapiens* Tim9-Tim10 complex) and 3DXR (*Saccharomyces cerevisiae* Tim9-Tim10 complex).

Figure S6

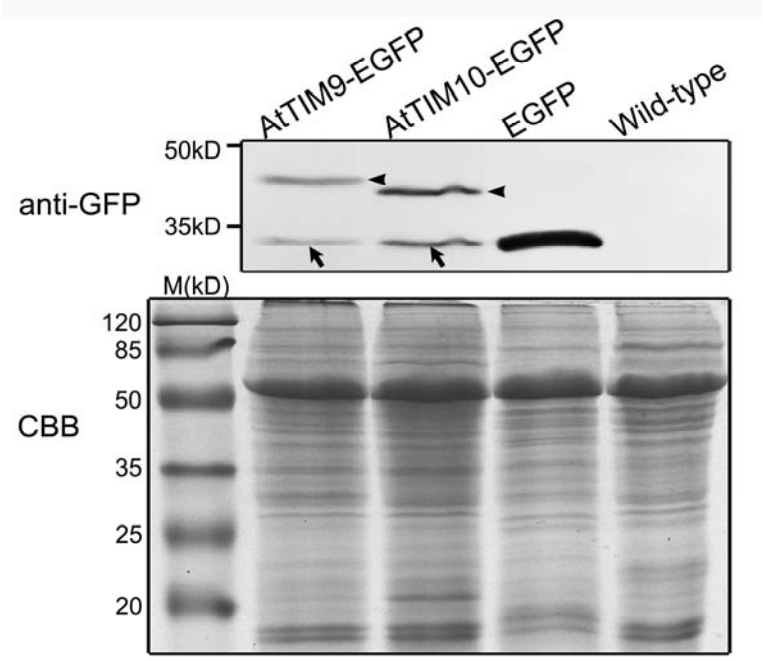

Figure S6 Immunoblot analysis of AtTIM9-EGFP and AtTIM10-EGFP fusion protein. Coomassie blue-stained gel (CBB) as a loading control. Molecular markers (M) are shown on the left. Arrowheads and arrows indicate the full-length AtTIM9-EGFP/AtTIM10-EGFP fusions and their degradative GFP, respectively.

Figure S7

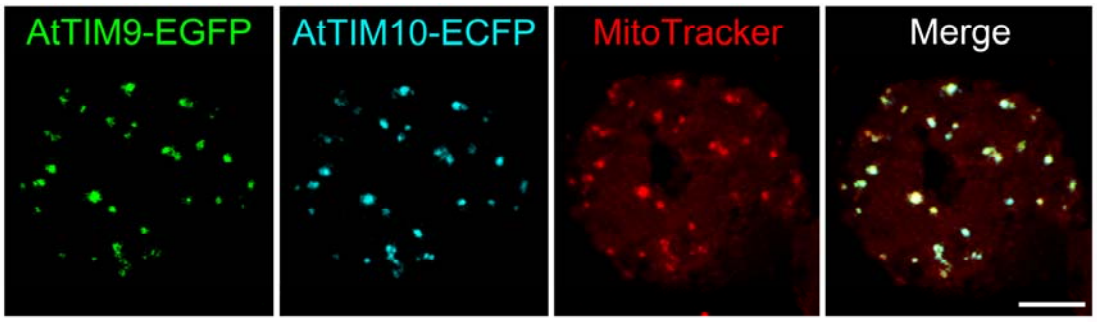

Figure S7 Co-localization of AtTIM9 and AtTIM10 in mitochondrial. AtTIM9-GFP and AtTIM10-CFP are co-localized with mitochondria in *Arabidopsis* protoplasts. Right panel shows the entire overlapping of EGFP, ECFP and MitoTracker channels. Bar = 10μm.

Supplemental Tables

Table S1 Transmission of the *tim9-1*, *tim9-2* and *tim10* mutants.

Cross (Female×Male) [a]	SM [b]	Resistant	Sensitive	R: S Rate [c]	Expected Rate	TE (Female) [e]	TE (Male) [e]
tim9-1/+ × +/+	Bas	210	212	1:1.01 [d]	1:1	99.1%	NA
+/+ × *tim9-1*/+	Bas	236	240	1:1.02 [d]	1:1	NA	98.3%
tim9-2/+ × +/+	Sul	244	263	1:1.08 [d]	1:1	92.8%	NA
+/+ × *tim9-2*/+	Sul	214	220	1:1.03 [d]	1:1	NA	97.3%
tim10/+ × +/+	Sul	121	125	1:1.03 [d]	1:1	96.8%	NA
+/+ × *tim10*/+	Sul	170	182	1:1.07 [d]	1:1	NA	93.4%

[a] Plants were crossed manually, and seeds of the resulting cross were collected and grown on selective plates to determine the efficiency in which the mutant allele was transmitted to the next generation by the male or female gametes.

[b] Selection marker (SM): BASTA (Bas) and Sulfadiazine (Sul).

[c] Resistant (R): Sensitive (S).

[d] Not significantly different from the segregation ratio 1:1 ($P > 0.05$).

[e] TE = Resistant/Sensitive × 100%.

Table S2 Primers (5' to 3') used in the experiments.

2.1 Primers for mutant verification		
	FP	RP
9-1	caggcccaataaagaaaatcgc	
9-2		tgacaacaacacacaaaatgagac
CSLB	cccatttggacgtgaatgtagacac	
161LB	atctgatttcccaacccaatc	
2.2 Primers for complementation		
	FP	RP
AtTIM9-F	cgAAGCTTaggcccaataaa gaaaatcgctagg	cgGTCGACtcccgtaaacttg aaaatctccatga
AtTIM10-F	atGTCGACaatggaccaaact catccaacgaaa	cgGGATCCaatatagatgtgttt cgttattttc
9	atcaacaatagtacaatgcaatt	tgacaacaacacacaaaatgagac
10	acccggatattgacctgttcaag	caaccttgtgctctaactgaagaa
2.3 Primers for GUS fusion constructs		
	FP	RP
AtTIM9-Pro-GUS	atGTCGACtatttttgagttag gtcatgagat	atAAGCTTgcCATttttttccc aactcttttct
AtTIM10-Pro-GUS	atGAATTCaatggaccaaactc atccaacgaaa	gcGTCGACCATttttttagca gtacctgaat
2.4 Primers for the ORF of AtTIM9 and AtTIM10		
	FP	RP
AtTIM9-ORF	actTCTAGAatggacgcaagc atgatggc	tcaGGATCCgtcttgggttggt gcgttctg
AtTIM10-ORF	actTCTAGAatggcttctcctat tcccgt	actGGATCCcacgggaggctt gccagcac
2.5 Primers for subcellular localization fusion constructs		
	FP	RP
AtTIM9-Pro-EGFP	actAAGCTTttttgagttaggtc atgagattgg	actTCTAGAttttttcccaactct tttctttc
AtTIM10-Pro-EGFP/ECFP	cgCTGCAGaatggaccaaact catccaa	cgCTGCAGttttttagcagtac ctgaat
CFP	atGGATCCatggtgagcaagg gcgagga	atGAGCTCttacttgtacagctc gtccatgc

2.6 Primers for qRT-PCR		
	FP	RP
GAPDH	gagtctactggtgtcttcactg	caaggtcggacttgtattcgtg
AtTIM9-qRT	ttggtggagaggtgtttcgtg	atcagtcttgggttggtgcg
AtTIM10-qRT	cacaaacggagatggagta	acggtcgatgcaactattc
2.7 Primers for in situ hybridization		
	FP	RP
AtTIM9-ISH-S	CATAATACGACTCACTATAGGGgtggagaggtgtttcgtgga	ttgggttggtgcgttctgatt
AtTIM9-ISH-AS	ggtggagaggtgtttcgtgga	CATAATACGACTCACTATAGGGttgggttggtgcgttctgatt
AtTIM10-ISH-S	CATAATACGACTCACTATAGGGtggcacaaacggagatggagt	ggaaacacaacggtcgatgca
AtTIM10-ISH-AS	tggcacaaacggagatggagt	CATAATACGACTCACTATAGGGggaaacacaacggtcgatgca
2.8 Primers for yeast two-hybrid		
	FP	RP
AtTIM9-AD	cgGAATTCgacgcaagcatgatggctgg	cgCTCGAGcgtcttgggttggtgcgttc
AtTIM9-BK	cgGAATTCgacgcaagcatgatggctgg	cgGGATCCcgtcttgggttggtgcgttc
AtTIM10-AD	cgGAATTCgcttctcctattcccgtcgg	cgCTCGAGccacgggaggctgccagca
AtTIM10-BK	cgGAATTCgcttctcctattcccgtcgg	cgGGATCCccacgggaggctgccagca
2.9 Primers for Co-IP		
	FP	RP
4MYC	atGGATCCatggaacaaaagctaatctc	atGAGCTCttacaagtcttcctcggaga

Supplemental Methods

Determination and comparison of protein structures

Based on Webb et al. (2006) had published the crystal structure of the human Tim9-Tim10 complex (Protein Data Bank code 2BSK), the structure of AtTIM9 and AtTIM10 could be built with molecular replacement by using the programs online (Eswar et al., 2003). Homology templates of AtTIM9 and AtTIM10 models were obtained by SWISS-MODEL and imported into Swiss-Pdb viewer 4.0.1 (Schwede et al., 2003), followed by processed steps to determinate the final models. Model refinement, visualization, and superposition were made by using Chimera 1.5.3 (Pettersen et al., 2004).

Construction and plant transformation

Vector construction was performed as described previously (Li et al., 2010). To see the GUS expression in *AtTIM9* and *AtTIM10* promoter reporter plants, the promoters of *AtTIM9* and *AtTIM10* were amplified and inserted into the *pCambia1381Xb* vector (Cambia) to form gene expression constructions: *ProAtTIM9::GUS* and *ProAtTIM10::GUS*. The primers used in these experiments are listed in Table S2.3.

To observe protein subcellular distributions, the operation procedure was described according to Ren et al. (2012). We first constructed the *pC1300-EGFP* and *pC2301-ECFP* empty vector (*pCambia1300*, *pCambia2301*; Cambia). And then, the promoter sequences and open reading frame (ORF) regions of *AtTIM9* and *AtTIM10* were also amplified and inserted into the rebuilt vectors to produce the final version of the subcellular localization constructions: *ProAtTIM9::AtTIM9-EGFP*, *ProAtTIM10::AtTIM10-EGFP*, and *ProAtTIM10::AtTIM10-ECFP*. Primers used in the experiments are listed in Table S2.4, 2.5.

After sequencing, all constructs were transformed into *Arabidopsis* (Col) by using the floral dip method. After screening on MS medium with 10 mg/L hygromycin, positive transformants were used for subsequent analysis. After PCR verification, the 3:1 segregating transformed lines were selected on plates, and then the homozygous lines screened in T3 generation were used for further experiments.

Histochemical GUS analysis

The procedure for histochemical GUS staining was described by Ren & Zhao (2009). After staining, the samples were observed under an OLYMPUS SZX12 stereomicroscope and photographed by OLYMPUS E330 digital camera. For detecting GUS expression in ovules, the GUS staining was carried out as described previously (Chen et al., 2010), and observed using the OLYMPUS BX60 microscope and photographed with a charge-coupled device (CCD) OLYMPUS DP72.

Supplemental Literature Cited

Chen D, Ren YJ, Deng YT, Zhao J (2010) Auxin polar transport is essential for the development of zygote and embryo in *Nicotiana tabacum* L. and correlated with ABP1 and PM H^+-ATPase activities. J Exp Bot **61**: 1853–1867

Eswar, N., John, B., Mirkovic, N., Fiser, A., Ilyin, V. A., Pieper, U., Stuart, A.C., Marti-Renom, M.A., Madhusudhan, M.S., Yerkovich, B., Sali, A (2003) Tools for comparative protein structure modeling and analysis. Nucleic Acids Res **31**: 3375–3380.

Li J, Yu M, Geng LL, Zhao J (2010) The fasciclin-like arabinogalactan protein gene, FLA3, is involved in microspore development of *Arabidopsis*. Plant J **64**: 482–497.

Pettersen, E.F., Goddard, T.D., Huang, C.C., Couch, G.S., Greenblatt, D.M., Meng, E.C., and Ferrin, T.E (2004) UCSF chimera - A visualization system for exploratory research and analysis. J Comput Chem **25**: 1605–1612.

Ren YJ, Liu Y, Chen HY, Li G, Zhang XL, Zhao J (2012) Type 4 metallothionein genes are involved in regulating Zn ion accumulation in late embryo and in controlling early seedling growth in *Arabidopsis*. Plant Cell Environ **35**: 770–789.

Ren YJ, Zhao J (2009) Functional analysis of the rice metallothionein gene OsMT2b promoter in transgenic *Arabidopsis* plants and rice germinated embryos. Plant Sci **176**: 528–538.

Schwede, T., Kopp, J., Guex, N., and Peitsch, M.C (2003) SWISS-MODEL: an automated protein homology-modeling server. Nucleic Acids Res **31**: 3381–3385.

Webb, C.T., Gorman, M.A., Lazarou, M., Ryan, M.T., and Gulbis, J.M (2006) Crystal structure of the mitochondrial chaperone TIM9•10 reveals a six-bladed α-propeller. Mol Cell **21**: 123–133.